Random walks and polygons in tight confinement

Y. Diao[1], **C. Ernst**[2] **& U. Ziegler**[2]

[1] Department of Mathematics and Statistics,
University of North Carolina Charlotte, Charlotte, NC 28223, USA
[2] Department of Mathematics and Computer Science,
Western Kentucky University, Bowling Green, KY 42101, USA

E-mail: ydiao@uncc.edu, claus.ernst@wku.edu, uta.ziegler@wku.edu

Abstract. We discuss the effect of confinement on the topology and geometry of tightly confined random walks and polygons. Here the walks and polygons are confined in a sphere of radius $R \geq 1/2$ and the polygons are equilateral with n edges of unit length. We illustrate numerically that for a fixed length of random polygons the knotting probability increases to one as the radius decreases to $1/2$. We also demonstrate that for random polygons (walks) the curvature increases to πn ($\pi(n-1)$) as the radius approaches $1/2$ and that the torsion decreases to $\approx \pi n/3$ ($\approx \pi(n-1)/3$). In addition we show the effect of length and confinement on the average crossing number of a random polygon.

1. Introduction

Many systems and processes in nature do not exist under ideal conditions, but are subject to constraints imposed by the environment in which they occur or the manner in which they are created. This article investigates polygonal random walks and random polygons that are constrained in a small volume. The study of such objects is motivated by physical entities that exist or are created within a small volume and that contain self-entanglements (knots or links). Such topologically and space constrained systems can be found in areas of biology, chemistry and physics. The two examples described below demonstrate the importance of studying such systems. Some macromolecular self-assembly processes pack DNA molecules in a highly condensed manner. For example, in the case of a human cell, the genome contains about 2 meters of DNA, all folded into the nucleus, which is a million times smaller in diameter. The ratio between the volume occupied by a given genome and the volume occupied by a random walk of the same length as the genome (if the genome were to be modeled by a random walk), generally ranges from 10^2 to 10^4 (Holmes & Cozzarelli, 2000). This process of compacting DNA molecules is often called DNA condensation and affects virtually every biological process involving DNA molecules (Horn & Peterson, 2000). Despite the important role that DNA packing mechanisms play in all living organisms and the efforts spent studying them, only some details are known about the workings of DNA packaging motors (Zhang *et al.*, 2012). The general packing mechanisms of double-stranded DNA (dsDNA) remain largely unknown even in the simplest organisms such as viruses like bacteriophages where DNA molecules are packed in a viral capsid (a bacteriophage is a virus that infects and replicates within bacteria). In the case of bacteriophages, the organization of the condensed DNA facilitates the process of DNA packing and provides stability to the capsid while packaged and also facilitates the release

of DNA upon infection. Important topological aspects of DNA packing are detected in DNA extracted from bacteriophage P4. These extracted circular DNA molecules are non-trivially knotted with very high probability (Liu *et al.*, 1981*a*,*b*). In particular, quantitative analysis of the knots extracted from bacteriophage P4 revealed that the DNA inside P4 is likely to be chirally organized (Arsuaga *et al.*, 2005). In (Marenduzzo *et al.*, 2009) a model is introduced that replicates successfully some aspects of the observed knot spectrum observed in these experiments.

Another motivation to study random walks and polygons arises in physics. In theoretical physics, quantum chromodynamics (QCD) is the theory of the actions of the strong force (color force), a fundamental force describing the interactions between quarks and gluons which make up hadrons (such as the proton, neutron or pion). The theory is an important part of the standard model of particle physics. A huge body of experimental evidence for QCD has been gathered over the years. In high-energy particle collision, the center of the collision forms a small superheated volume of hot plasma which contains quarks, antiquark and gluons. In a model proposed by physicists (Buniy & Kephart, 2003; Buniy *et al.*, 2013) knots and links play a central role. As the plasma cools the particles rehadronize to form mesons and baryons, and in this process chromoelectric flux tubes can form that may close into knots and links. The spectrum of tight knotted and linked flux tubes in QCD are the observed f_J states seen in high-energy experiments (Buniy *et al.*, 2013). Confinement arises because the knotted flux tubes are confined in the volume of the superheated plasma.

In both examples, one or more (the latter in the case of the quantum flux) tube- or chainlike, self-closing (circular) structures are created or packed inside a confining volume. This creates structures that contain non-trivial self-entanglements (expressed as knots and links). The packing process cannot be observed directly, and experiments (and simulations) provide only scattered snapshots and evidence of the activity. A potential packing mechanism under investigation may only be valid if its simulation produces results that are (statistically) consistent with those observed in experiments. The data reported in this article presents observable packing results for a random packing mechanism. This article is structured as follows: In Section 2 we provide the necessary background terminology in topology and geometry. In Section 3 we give a brief introduction to the generation of random walks and polygons. In Sections 4.1, 4.2 and 4.3 we discuss the numeric data on curvature, torsion, average crossing number and knotting probabilities. Finally, in section 5 we describe future work and state some open questions.

2. Background

The random rope-like physical structures such as the ones encountered in the above examples are modeled in this study as equilateral random polygons confined inside a sphere of a fixed radius R. This section provides important background information about topics related to topology and geometry. Many of these terms can be found in any standard book in knot theory such as (Adams, 2004; Burde & Zieschang, 2002; Cromwell, 2004). The topology of a polygon is expressed by the different knots that can be formed in the polygon. Mathematically, a knot is a just simple closed curve in $\mathbb{R}^3$. Intuitively, two knots are considered topologically equivalent if one can continuously deform one to the other without breaking the curve or causing self-intersections. A *knot type* is defined as the set of all topologically equivalent knots. We use the symbol K when referring to a particular member of the knot type $\mathcal{K}$. A *knot diagram* D is the projection of a knot K onto a plane. D is *regular* if no more than two segments of K cross at the same point in the projection. At each intersection one of the strands of the knot K is below or above the other strand. An intersection in a regular projection is called a *crossing*. The minimum number of crossings taken over all regular projections of all members from a knot type $\mathcal{K}$ is called the *crossing number* of the knot type $\mathcal{K}$ and is denoted by $Cr(\mathcal{K})$. A diagram of $\mathcal{K}$ that realizes the crossing number of $\mathcal{K}$ is called a *minimal diagram*. Figure 1 shows two knot

diagrams that look very much alike but are not. A *knot invariant* of a knot type $\mathcal{K}$ is a quantity Q (such as a number or a polynomial or a group) that can be computed (usually using a knot diagram) with the following property: If K and L are two knots of the same knot type $\mathcal{K}$ then $Q(K) = Q(L)$. Thus if for two knots K and L the knot invariant is different ($Q(K) \neq Q(L)$) then K and L represent different knot types. However the converse of this statement is not true.

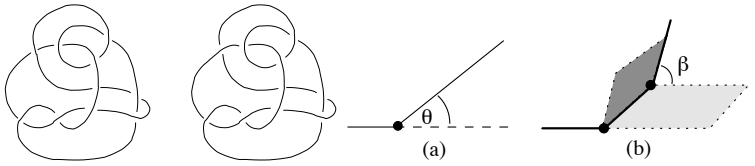

Figure 1. On the left: Two non-minimal knot diagrams: The left one simplifies to the eight-crossing knot 8_9 in the knot table (Cromwell, 2004) while the right one simplifies to the unknot. On the right: (a) and (b): The angles used to define the total curvature and total torsion of a polygon

Different packing mechanisms affect the overall geometric properties of the random walks and polygons (to be defined in Section 3.1). Note that these geometric quantities are not topological invariants, their value depends on the particular chosen polygonal representative. However these geometric quantities are well suited to describe a collection of random walks and polygons by taking the average value over all members of the collection. Below we define some simple geometric quantities that we discuss in this article. Any two consecutive edges of a given polygon define an angle θ as shown in Figure 1(a). Notice that $0 \leq \theta \leq \pi$. The *total curvature* of the polygon is defined as the sum of all these angles. Any two consecutive edges of a given polygon define a plane when the two edges are not co-linear. The two planes defined by three consecutive edges define a torsion angle β such that $0 \leq \beta \leq \pi$ as shown in Figure 1(b). The *total torsion* of the polygon is defined as the sum of all these torsion angles. The *average crossing number* (or ACN) of a polygon is the average number of crossings over all possible diagrams (or projection) of the polygon. (The ACN should not be confused with the crossing number of a knot type.)

3. Equilateral Random Walks/Polygons

Equilateral random walks/polygons are the simplest and most fundamental type of random walks/polygons which are composed of freely jointed segments of equal length.

3.1. Unconfined Random Walks/Polygons

Let $\vec{r}_k$, $k = 1, 2, ..., n$ be n independent random unit vectors uniformly distributed on the unit sphere centered at the origin O. An equilateral random walk W_n of length n is then defined as the piece-wise linear path whose vertices are given by $X_0 = O$, $X_k = \vec{r}_1 + \vec{r}_2 + \cdots + \vec{r}_k$ $(1 \leq k \leq n)$. An equilateral random polygon of length n is then defined as an equilateral random walk of length n subjected to the condition $X_n = O$. Equilateral random walks/polygons consist of individual segments which have no thickness. Such a random walk/polygon is also known as an ideal random walk/polygon and it was already used to model the behavior of chain polymers/closed chain polymers under the so-called theta conditions (where polymer segments that are not in direct contact neither attract nor repel each other) in the middle of last century by Flory and de Gennes (Flory, 1953; Gennes, 1979). This is a subject that had been extensively studied. Much is known about the overall behavior of equilateral random walks/polygons. For example, the overall dimensions such as the average end-to-end distance or the average radius of gyration is known to scale with the number of segments n as $\sqrt{n}$ (Doi & Edwards, 1986; Flory, 1953;

Gennes, 1979; Zirbel & Millett, 2012), the average crossing number grows as $O(n \ln(n))$ (Diao *et al.*, 2003) and the average squared writhe is believed (with numerical and partial analytical evidence) to grow as $O(n)$ (Portillo *et al.*, 2011). Moreover, there are several generating methods that are well tested and efficient in generating random equilateral polygons such as the hedgehog method (Dobay *et al.*, 2003), the crankshaft method (Klenin *et al.*, 1988; Millett, 2000), or the generalized hedgehog method (Varela *et al.*, 2009). These methods are all well tested and believed to generate non-correlated samples of equilateral random polygons. In the case of the generalized hedgehog method (developed by one of the authors), an equilateral random polygon of length n can be generated in $O(n)$ time (Varela *et al.*, 2009).

3.2. Confined Equilateral Random Walks/Polygons

Unlike the unconfined case, generating confined equilateral random polygons is more difficult. In this project and all the related references cited here, the confining space (volume) is modeled by a sphere S_R of radius $R > 0.5$. (A sphere S of radius $R < 0.5$ cannot contain any segments of unit length.) If one uses an accept/reject approach with any one of the methods mentioned in section 3.1, namely accepting only those unconfined random walks/polygons generated that are contained in S, then the computation time grows exponentially with the length of the walks/polygons. Recently the authors have developed several methods to efficiently generate confined equilateral random polygons using probability density functions at each step of the generation process (Diao *et al.*, 2011, 2012*a*,*b*). These methods have several advantages: first, they can generate random polygons efficiently even in tight confinement, and secondly they allow a theoretical analysis on geometric properties of the polygons generated.

At a first glance, a confined equilateral random walk/polygon just means an equilateral random walk/polygon subjected to the condition that it is within the confining sphere S and the matter seems to be just how to apply this condition in the generating process (from a numerical analysis point of view). However, closer examinations reveal that the matter is more complicated. First, there is no reason why the walk or the polygon has to be rooted at the center of S or at any particular point in S. This is different from the case of the unconfined equilateral random walks/polygons where all walks/polygons are rooted at the origin O (since one can always move the starting point of the walk/polygon to the origin through translation without changing the relative relations of the edges along the walk/polygon). In general, one has to choose the starting point of the random walk/polygon according to a certain probability distribution of the vertices. Second, once the starting point of the random walk/polygon is chosen, the random walk/polygon is an equilateral random walk/polygon subject to the condition that the entire walk/polygon has to stay within S. It turns out that there are different ways to impose this condition leading to random walks/polygons with different probability distributions for the distances of vertices to the center of the sphere.

Despite its apparent importance with many potential applications, the confined equilateral random walks/polygons have received little attention in the past. Consequently, there have been no systematic study on this subject until the recent results by the authors (Diao *et al.*, 2011, 2012*a*,*b*). The following are two different ways to impose (define) the confining condition on a random walk/polygon that have been discussed in their work.

Let n be the length of the equilateral walk/polygon, and let X_0 be the starting point of the walk/polygon with X_1, X_2, ..., X_{n-1}, X_n being the other vertices on the walk/polygon, labeled according to their order along the walk/polygon. In the case of the polygon, $X_n = X_0$. Assume that the distribution of X_0 is given and that X_0 has been chosen according to this distribution. The random walk/polygon is defined in an iterative manner in both definitions.

Condition R. Assuming that X_k has been selected, then the next vertex X_{k+1} is selected subject to the conditions that X_k, X_{k+1}, X_{k+2}, ..., X_n form an equilateral random walk with fixed end point X_k and X_{k+1} is within the confining sphere S (In the case of a polygon we must

also have $X_n = X_0$) .

Condition A. Assuming that X_k has been selected, then the next vertex X_{k+1} is selected subject to the conditions that X_k, X_{k+1}, X_{k+2}, ..., X_n form an equilateral random walk with fixed end point X_k such that this random walk is entirely contained in S. (In the case of a polygon we must also have $X_n = X_0$) .

Both conditions can be used to generate confined equilateral random walks/polygons and generate the un-confined equilateral random walks/polygons once the confining condition is removed (by setting $R = \infty$). Condition A is equivalent to the following (Diao *et al.*, 2012*a*): Suppose we generate random polygons ignoring the confinement condition and starting at the origin. Out of all the polygons generated we now only keep those that lie in confinement. This is often called an absorbent boundary, any polygon that penetrates the boundary is absorbed (i.e. it vanishes). The letter R is referring to the fact that the confining sphere acts in a way similar to a reflective surface: a polygons hitting the boundary is reflected back into the confining sphere. The two conditions lead to different distributions of random walks/polygons. This is illustrated by Figure 2 which shows an example of two different vertex density distributions generated by the two conditions in the special case of $R = 1.5$, $n = 20$ and $X_0 = O$. More specifically Figure 2 shows the distances of each vertex X_i to the origin O for $3 \leq i \leq n-3$ and the histogram has been normalized to represent a probability density function. The lighter (yellow) shading corresponds to Definition R and darker (blue) shading corresponds to Definition A.

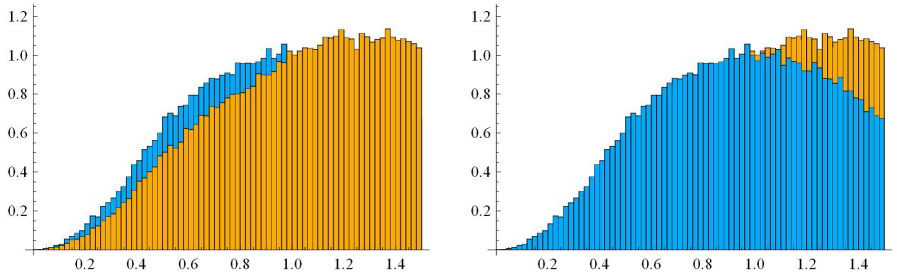

Figure 2. Probability density functions for the distances to the center of the sphere for the vertices of 20-step polygons rooted at the center of the confining sphere with $R = 1.5$. The lighter shading is for Definition R and the darker for Definition A.

4. The Effect of confinement

4.1. Mean Total Curvature and Torsion

It is quite intuitive that confined random walks (polygons) have expected total curvature values larger than their unconfined counterparts since the confinement condition forces the random walks (polygons) to make sharper and more frequent turns on average. In the extreme case the confinement sphere has a diameter close to the unit edge length, and the random walk (polygon) has to make a near 180 degree turn at each step. Hence its average total curvature would be close to $(n-1)\pi$ (or $n\pi$ for a polygon) where n is the number of vertices. On the other hand, if the confinement radius is very large relative to the edge length, then the walk (or polygon) behaves like it is unconfined. In this case the average curvature per edge approaches $\pi/2$ as $n \to \infty$ for both the random walks and the random polygons. However the random polygons have slightly larger mean total curvatures than the random walks. For large n, the mean total curvature of the unconfined random polygons of n edges is approximately $n\pi/2 + 3\pi/8$, while the mean total curvature of the unconfined random walks of n edges is precisely $(n-1)\pi/2$ (Grosberg, 2008). These two simple cases demonstrate that the extreme confinement condition

can almost double the expected curvature. The left side of Figure 3 is a numerical comparison the mean curvatures per edge between a random walk and a random polygon with $n = 60$. Clearly we can see that the polygons have a slightly larger curvature due to the correction term of $3\pi/8$. In fact, expressed per edge this term is $\pi/160 \approx .02$. Lowering the squares representing the polygons by this amount would show the two data sets matching almost perfectly. (For the radii where we have both data points the mean difference between the two sets is $\approx .014$.)

It is much less intuitive why a confined random walk (or polygon) would have an expected torsion smaller than that of its unconfined counterpart. Again let us look at the two extreme cases. If the confinement radius is very large relative to the edge length, then the walk (or polygon) behaves as an unconfined one. In this case the average torsion per edge approaches $\pi/2$ as $n \to \infty$ (for both the random walks and the random polygons), though a random polygon has a slightly smaller average torsion than a random walk does. As $n \to \infty$, the average total torsion of an unconfined random polygon approaches $n\pi/2 - 3\pi/8$ (Grosberg, 2008). In the case of tight confinement, our numerical results show that the average torsion per edge is smaller than $\pi/2$ per edge. In fact, our numerical results strongly support the following conjecture:

Conjecture: As $n \to \infty$ and $R \to 1/2$, the average torsion (per edge) of a random walk (polygon) of n edges approaches $\pi/3$.

See the right side of Figure 3. Here we see that the polygons have a slightly smaller torsion due to the correction term $-3\pi/8$. As above, expressed per edge this term is $\pi/160 \approx .02$ and raising the squares representing the polygons by this amount would show the two data sets matching almost perfectly. (For the radii where we have both data points the mean difference between the two sets is $\approx .02$.) At this point a rigorous proof of this conjecture is elusive, and certainly seems difficult. The authors believe that a careful analysis of an integral expression of the average torsion might be possible for the case of a random walk. However for a random polygon this seems extremely difficult if not impossible. As a final remark we want to point out that the data shown in Figure 3 suggest that random walks and polygons in confinement have very similar values with respect to their mean curvature and torsion values. This is a little misleading. In fact, the length of the polygon also plays a role here. If the random polygons are relatively short with respect of the confinement condition then it might only barely reach the boundary and the confinement plays no role. If the random polygon is very long then we know that the vertex distribution of the random polygon (generated using Condition A) does not match the vertex distribution of the random walk, see Figure 2 and thus there might be a difference between the torsion and curvature values of random walks and random polygons that does not get smaller as the length of the walks and polygons increases. Finally, we should also point out that when R is close to $1/2$, the confined random polygons have to have even length (unless the polygon is very long): the equilateral triangle is the simplest example of a random polygon of odd length that cannot be confined in a sphere of radius close to $1/2$.

4.2. Mean Average Crossing Number (ACN)

A standard measure of the geometric complexity of random polygons is their mean average crossing number (mean ACN). Figure 4 shows the mean ACN of polygons ranging in length from 10 to 90 with radii of confinement ranging from $R = 1$ to $R = 4.5$, with a clear indication on how tight confinement leads to a drastic increase in the mean ACN. In (Diao *et al.*, 2011; Arsuaga *et al.*, 2009; Diao *et al.*, 2012*a*) the mean ACN is modeled by a best fit-function of the form $y = a(R)n^2 + b(R)n\ln(n)$, where $a(R)$ and $b(R)$ are constants that depend on the radius of confinement R. Using this model we fit the data to a function of the type

$$f(x, y) = \left(a + \frac{b}{x^2}\right) y^2 + \left(c + \frac{d}{x^2}\right) y \ln(y),$$

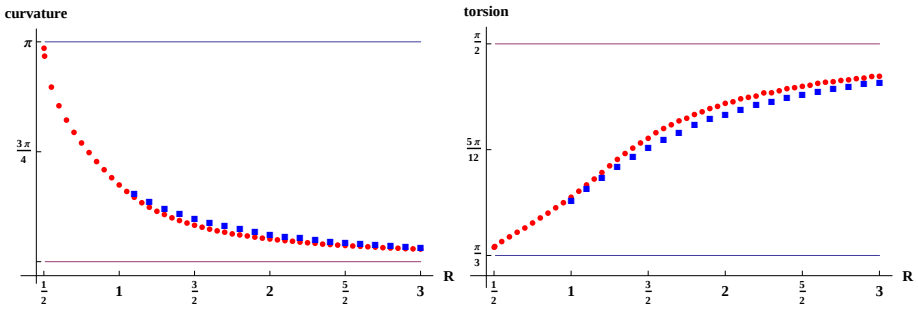

Figure 3. Curvature (on the left) and torsion (on the right) per edge: The squares represent random polygons of length 60 and the dots represent a single random walk of length one million. The confinement radii (on the x-axis) vary from 1/2 to 3. The random polygons are generated under Condition A using the methods of (Diao *et al.*, 2012*a*): Each data point for the polygons is based on a sample of size 10,000 while each data point for the random walks is based on a single walk with one million edges generated under Condition R.

where the x variable models the confinement radius R and the y variable models the polygon length. We found that values of $a \approx 0.0005$, $b \approx 0.12$, $c \approx 0.052$ and $d \approx 0.126$ give an excellent fit with an R^2-value of 0.999978 and a mean difference between the best-fit function and the data of less than 0.35.

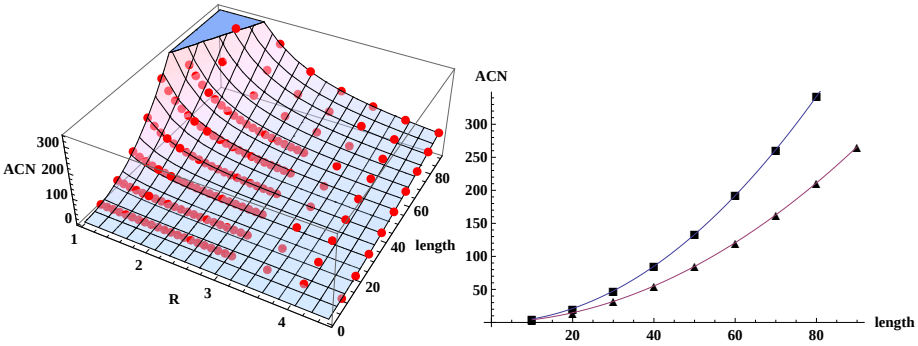

Figure 4. The mean ACN in a 3D plot (on the left) and two slices through the surface for radii $R = 1.5$ (■) and $R = 2$ (▲). Each data point is obtained from a sample of 10,000 polygons.

One interesting question here is whether the mean ACNs of knotted and unknotted random polygons are different. A positive answer to this question implies that one may use the mean ACN of certain random polygons to make inferences about their topological properties such as their knotting probabilities (which is addressed in the next section). Figure 5 shows the numerical estimation of the ratio (for each fixed length and radius) between the mean ACN of the knotted random polygons and the mean ACN of all random polygons. As expected this ratio is greater than one for all data points. Furthermore, the shorter the polygons and the larger the confining radii, the larger the ratios. We interpret this data as follows: In shorter polygons with a larger confinement radius where knotting is less likely, the ACN of a knotted polygon is higher than the ACN of an unknotted polygon on the average because the topological complexity imposes an increased geometric complexity. The ACN ratio for unconfined random polygons is larger than 1 due to the same reason. With increased length and/or decreased confinement

radius, the probability of knotting increases as does the number of crossings in diagrams of unknotted polygons and hence the knotting complexity no longer results in a much increased ACN, causing a much smaller difference and a smaller ratio. To illustrate this we give a few examples: For length ten and radius one we get a ratio of ≈ 1.27 which increases to ≈ 2.18 for radius three. For length forty and radius one we get a ratio of ≈ 1.002 which increases to ≈ 1.17 for radius three. The noisy results for polygons of length ten at higher confinement radii are due to the fact that there were very few knotted polygons in these ranges. Much larger sample sizes may be needed in order to reduce the noise.

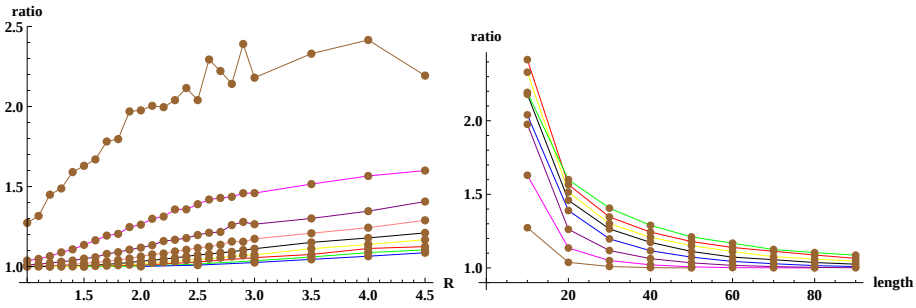

Figure 5. The ratio of the average crossing number of knotted random polygon over the average crossing number of all random polygons. Left: The radius R is on the x-axis and there are nine curves representing the lengths of the polygons ranging from 10 (on the top) to 90 (at the bottom). Right: The lengths of the polygons is on the x-axis and there are eight curves for various values of R from 1 (bottom) to 4.5 (top) in increments of 1/2.

4.3. Knotting Probabilities

The famous Frisch-Wasserman-Delbrück conjecture states that sufficiently long ring polymers should be knotted with probability one (Frisch & Wasserman, 1961; Delbruck, 1962). This conjecture has been proven for several models of polymer rings including the (unconfined) equilateral random polygons (Diao, 1995). While it is very intuitive and plausible that this conjecture is also true for confined (equilateral) random polygons, no one has been able to prove it to date. The left of Figure 6 shows the numerical estimations of the knotting probabilities using the same random polygon sample used in Figure 3. The nine fitting curves represent polygons of lengths ranging from 10 to 90 with increments of 10. All the random polygons shown are generated under Condition A (Diao *et al.*, 2012*a*) and are rooted at the origin (thus the confinement radius cannot be less than one). Knotting was determined by a calculation of the HOMFLY polynomial. For long polygons and small radii R this polynomial computation becomes impossible due to the complexity of the calculation. The unknotting probabilities for $R = 1$ and $R = 1.5$, $n = 10$, 20, 30, 40 and 50 are shown at the right side of Figure 6. At length $n = 50$, most polygons are knotted at $R = 1$ and $R = 1.5$. This shows how drastically the confinement can increase the knotting probability: only about 20% of unconfined equilateral random polygons at length 50 are knotted and this percentage increases to only 50% at length 500 (Millett & Rawdon, 2005).

5. Conclusions

In this paper, we demonstrated, using numerical simulations, the effect of volume confinement on several important geometric measures of random polygons including the mean total curvature, mean total torsion and mean total ACN. We also investigated the effect of volume confinement

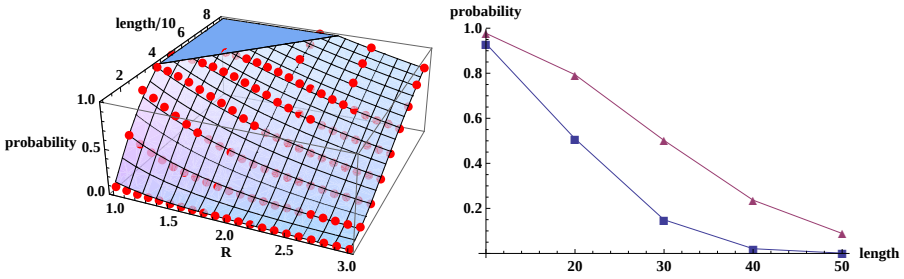

Figure 6. Left: the knotting probability with the confinement radii (x-axis) vary from 1 to 3 and the length (on the y-axis) varies from 10 to 90; Right: the unknotting probability for confinement radii $R = 1$ (■) and $R = 1.5$ (▲) and length $n = 10$, 20, 30, 40 and 50. Each data point is based on a sample of $10,000$ polygons.

to the knotting probabilities of random polygons of various lengths. Our results show that confinement leads to increased mean total curvature, but to a decreased mean total torsion. Our study of the overall mean ACN matches well with previously published results, but further reveals that for a fixed length, the confinement also elevates the ratio between the mean ACN of knotted polygons and the mean ACN of all polygons. As we pointed out in the introduction section, generating confined equilateral random polygons itself is a difficult problem. There are different ways to define and generate such confined random polygons. How these different definitions and generating methods affect these geometric or topological properties of the polygons is a question for a future study.

Let us end this paper with some open questions. Although our numerical results seem to favor a positive answer for each of them, a theoretical proof for any of these will not be easy.

1. For any fixed confinement radius R, the knotting probability of a random polygon of length n goes to 1 as $n \to \infty$;

2. For any suitably large n, the knotting probability of a confined random polygon of length n goes to 1 as $R \to 1/2$;

3. The total torsion of a confined random walk of n edges goes to $(n-1)\pi/3$ as $R \to 1/2$;

4. If n is even, then the total torsion of a confined random polygon of n edges goes to $n\pi/3$ as $R \to 1/2$.

Acknowledgments

Y. Diao is supported in part by NSF Grants #DMS-0920880 and #DMS-1016460, and C. Ernst and U. Ziegler are supported in part by NSF grant #DMS-1016420. The authors want to thank Eric Rawdon for his work in determining the HOMFLY polynomial for many of the polygons and determining their knot types.

References

Adams, C. 2004 **The Knot Book**. American Mathematical Society.

Arsuaga, J., Borgo, B., Diao, Y. & Scharein, R. 2009 The growth of the mean average crossing number of equilateral polygons in confinement. *J. Phys. A: Math. Theor.* **42**, 465202.

Arsuaga, J., Vazquez, M., McGuirk, P., Trigueros, S., Sumners, D. W. & Roca, J. 2005 Dna knots reveal a chiral organization of dna in phage capsids. *Proc. Natl. Acad. Sci. USA* **102**, 9165–9169.

Buniy, R. V., Cantarella, J., Kephart, T. W. & Rawdon, E. 2013 The tight knot spectrum in qcd. *preprint* .

Buniy, R. V. & Kephart, T. W. 2003 A model of glueballs. *Physics Letters B* **576**, 127–134.

Burde, G. & Zieschang, H. 2002 **Knots, Revised edition**. de Gruyter.

Cromwell, P. 2004 **Knots and Links**. Cambridge University Press.

Delbruck, M. 1962 Mathematical problems in the biological sciences. *Proceeding of the Symposium on Applied Mathematics, Vol. 14 (American Mathematical Society, Providence, RI, 1962)* **83**.

Diao, Y. 1995 The knotting of equilateral polygons in $\mathbb{R}^3$. *J. of Knot Theory and its Ramifications* **4**, 189–196.

Diao, Y., Dobay, A., Kusner, R., Millett, K. & Stasiak, A. 2003 The average crossing number of equilateral random polygons. *J. Phys. A: Math. Theor.* **36**, 11561–11574.

Diao, Y., Ernst, C., Montemayor, A. & Ziegler, U. 2011 Generating equilateral random polygons in confinement. *J. Phys. A: Math. Theor.* **44**, 405202.

Diao, Y., Ernst, C., Montemayor, A. & Ziegler, U. 2012*a* Generating equilateral random polygons in confinement ii. *J. Phys. A: Math. Theor.* **45**, 275203.

Diao, Y., Ernst, C., Montemayor, A. & Ziegler, U. 2012*b* Generating equilateral random polygons in confinement iii. *J. Phys. A: Math. Theor.* **45**, 465003.

Dobay, A., Dubochet, J., Millett, K., Sottas, P.-E. & Stasiak, A. 2003 Scaling behavior of random knots. *Proc Natl Acad Sci USA* **100**, 5611–5615.

Doi, M. & Edwards, S. 1986 **The theory of polymer dynamics**. Oxford University Press.

Flory, P. 1953 **Principles of Polymer Chemistry**. Cornell University Press.

Frisch, H. L. & Wasserman, E. 1961 Chemical topology. *J. Amer. Chem. Soc.* **83**(18), 3789–3795.

Gennes, P. G. D. 1979 **Scaling Concepts in Polymer Physics**. Cornell University Press.

Grosberg, A. Y. 2008 Total curvature and total torsion of a freely jointed circular polymer with $n >> 1$ segments. *Macromolecules* **41**(12), 4524–4527.

Holmes, V. F. & Cozzarelli, N. R. 2000 Closing the ring: links between smc proteins and chromosome partitioning, condensation, and supercoiling. *Proc. Natl. Acad. Sci. USA* **97**, 1322–1324.

Horn, P. J. & Peterson, C. L. 2000 Chromatin higher order folding: Wrapping up transcription. *Science* **297**, 1824–1827.

Klenin, K. V., Vologodskii, A. V., Anshelevich, V. V., Dykhne, A. M. & Frank-Kamenetskii, M. D. 1988 Effect of excluded volume on topological properties of circular dna. *J. Biomolec. Str. and Dyn.* **5**, 1173–1185.

Liu, L. F., Davis, J. L. & Calendar, R. 1981*a* Novel topologically knotted dna from bacteriophage p4 capsids: studies with dna topoisomerases. *Nucleic Acids Res.* **9**, 3979–3989.

Liu, L. F., Perkocha, L., Calendar, R. & Wang, J. C. 1981*b* Knotted dna from bacteriophage capsids. *Proc. Natl. Acad. Sci. USA* **78**, 5498–5502.

Marenduzzo, D., Orlandini, E., Stasiak, A., Sumners, D. W., Tubiana, L. & Micheletti, C. 2009 Dna-dna interactions in bacteriophage capsids are responsible for the observed dna knotting. *Proc Natl Acad Sci. USA* **106**(52), 22269–22274.

Millett, K. 2000 Monte Carlo explorations of polygonal knot spaces. *Proceedings of the International Conference on Knot Theory and its Ramifications held in Delphi, 1998*, Ser. Knots Everything **24**, 306–334.

Millett, K. & Rawdon, E. 2005 Universal characteristics of polygonal knot probabilities. *Jorge Alberto Calvo, Kenneth C. Millett, Eric J. Rawdon, and Andrzej Stasiak, editors*

Physical and Numerical Models in Knot Theory, Ser. Knots Everything, River Edge, NJ, World Sci. Publishing. **36**, 247–274.

Portillo, J., Arsuaga, J., Diao, Y., Scharein, R. & Vazquez, M. 2011 On the mean and variance of the writhe of random polygons. *J. Phys. A: Math. Theor.* **44**, 275004.

Varela, K., Hinson, K., Arsuaga, J. & Diao, Y. 2009 A fast ergodic algorithm for generating ensembles of equilateral random polygons. *J. Phys. A: Math. Theor.* **42**(9), 1–13.

Zhang, H., Schwartz, C., Donatis, G. M. D. & Guo, P. 2012 "push through one-way valve" mechanism of viral dna packaging. *Adv Virus Res.* **83**, 415–465.

Zirbel, L. & Millett, K. 2012 Characteristics of shape and knotting in ideal rings. *J. Phys. A: Math. Theor.* **45**, 225001.

Subject index

Frisch-Wasserman-Delbrück conjecture, 8

geometric properties, 3
    average crossing number ACN, 3
    curvature, 3
    torsion, 3

knot, 2
    crossing number, 2
    diagram, 2
    knot invariant, 3
    minimal diagram, 2

random polygon
    average crossing number ACN, 6
    knotting probability, 8
random walk/polygon, 3
    average crossing number ACN, 6
    confined, 4, 5
    confinement conditions, 4
    curvature, 5
    equilateral, 3
    torsion, 6
    unconfined, 5

Author index

Adams, C., 2
Anshelevich, V. V., 4
Arsuaga, J., 2, 4, 6

Borgo, B., 6
Buniy, R. V., 2
Burde, G., 2

Calendar, R., 2
Cantarella, J., 2
Cozzarelli, N. R., 1
Cromwell, P., 2, 3

Davis, J. L., 2
De Donatis, G. M., 1
De Gennes, P. G., 3
Delbruck, M., 8
Diao, Y., 1, 4–8
Dobay, A., 4
Doi, M., 4
Dubochet, J., 4
Dykhne, A. M., 4

Edwards, S.F., 4
Ernst, C., 1, 4–8

Flory, P., 3
Frank-Kamenetskii, M. D., 4
Frisch, H. L., 8

Grosberg, A. Y. , 5, 6
Guo, P., 1

Hinson, K., 4
Holmes,V. F., 1
Horn, P. J., 1

Kephart, T. W., 2
Klenin, K. V., 4
Kusner, R., 4

Liu, L. F., 2

Marenduzzo, D., 2
McGuirk , P., 2
Micheletti, C., 2
Millett, K., 4, 8
Montemayor, A., 4–8

Orlandini, E., 2

Perkocha, L., 2

Peterson, C. L., 1
Portillo, J., 4

Rawdon, E., 2, 8
Roca, J., 2

Scharein, R., 4, 6
Schwartz, C., 1
Sottas, P-E., 4
Stasiak, A., 2, 4
Stasiak, S., 4
Sumners, D. S., 2
Sumners, D. W., 2

Trigueros, S., 2
Tubiana, L, 2

Varela, K. R., 4
Vazquez, M., 2, 4
Vologodskii, A. V., 4

Wang, J. C., 2
Wasserman, E., 8

Zhang, H., 1
Ziegler, U., 1, 4–8
Zieschang, H., 2
Zirbel, L., 4